

1
2
3
4
5

6 **Probability Distribution Function of the Upper 7 Equatorial Pacific Current Speeds**

8
9
10

11
12 Peter C. Chu
13 Department of Oceanography
14 Naval Postgraduate School, Monterey, CA, 93493

15
16

Report Documentation Page			Form Approved OMB No. 0704-0188	
<p>Public reporting burden for the collection of information is estimated to average 1 hour per response, including the time for reviewing instructions, searching existing data sources, gathering and maintaining the data needed, and completing and reviewing the collection of information. Send comments regarding this burden estimate or any other aspect of this collection of information, including suggestions for reducing this burden, to Washington Headquarters Services, Directorate for Information Operations and Reports, 1215 Jefferson Davis Highway, Suite 1204, Arlington VA 22202-4302. Respondents should be aware that notwithstanding any other provision of law, no person shall be subject to a penalty for failing to comply with a collection of information if it does not display a currently valid OMB control number.</p>				
1. REPORT DATE 2005	2. REPORT TYPE	3. DATES COVERED 00-00-2005 to 00-00-2005		
4. TITLE AND SUBTITLE Probability Distribution Function of the Upper Equatorial Pacific Current Speeds			5a. CONTRACT NUMBER	
			5b. GRANT NUMBER	
			5c. PROGRAM ELEMENT NUMBER	
6. AUTHOR(S)			5d. PROJECT NUMBER	
			5e. TASK NUMBER	
			5f. WORK UNIT NUMBER	
7. PERFORMING ORGANIZATION NAME(S) AND ADDRESS(ES) Naval Ocean Analysis and Prediction Laboratory, Department of Oceanography, Naval Postgraduate School, Monterey, CA, 93943			8. PERFORMING ORGANIZATION REPORT NUMBER	
9. SPONSORING/MONITORING AGENCY NAME(S) AND ADDRESS(ES)			10. SPONSOR/MONITOR'S ACRONYM(S)	
			11. SPONSOR/MONITOR'S REPORT NUMBER(S)	
12. DISTRIBUTION/AVAILABILITY STATEMENT Approved for public release; distribution unlimited				
13. SUPPLEMENTARY NOTES				
14. ABSTRACT				
15. SUBJECT TERMS				
16. SECURITY CLASSIFICATION OF:			17. LIMITATION OF ABSTRACT Same as Report (SAR)	18. NUMBER OF PAGES 18
a. REPORT unclassified	b. ABSTRACT unclassified	c. THIS PAGE unclassified		

Abstract

The probability distribution function (PDF) of the upper (0-50 m) tropical Pacific current speeds (w), constructed from hourly ADCP data (1990-2007) at six stations for the Tropical Atmosphere Ocean project, satisfies the two-parameter Weibull distribution reasonably well with different characteristics between El Nino and La Nina events: In the western Pacific, the PDF of w has a larger peakedness during the La Nina events than during the El Nino events; and vice versa in the eastern Pacific. However, the PDF of w for the lower layer (100-200 m) does not fit the Weibull distribution so well as the upper layer. This is due to the different stochastic differential equations between upper and lower layers in the tropical Pacific. For the upper layer, the stochastic differential equations, established on the base of the Ekman dynamics, have analytical solution, i.e., the Rayleigh distribution (simplest form of the Weibull distribution), for constant eddy viscosity K . Knowledge on PDF of w during the El Nino and La Nina events will improve the ensemble horizontal flux calculation, which contributes to the climate studies.

Keywords: Probability distribution function, Ocean current speeds, Weibull distribution

14 Keywords: Probability distribution function, Ocean current speeds, Weibull distribution

1

2 **1. Introduction**

3 Tropical Pacific Ocean contributes significantly to the global redistribution of heat
4 necessary to maintain the earth's thermal equilibrium. For example, the El Niño (La Niña)
5 phenomenon, an eastward (westward) shift of warm (cool) water, is a key component of global
6 interannual climate variability. In connection with the El Niño and La Niña phenomena, impact
7 of upper tropical Pacific on global climate changes has attracted large attention. During the El
8 Niño or La Niña event, equatorial currents take an active role in redistribution of heat that
9 changes the sea surface temperature (SST) and in turn affects the atmospheric general
10 circulations.

11 Surface layer horizontal fluxes of momentum, heat, water mass and chemical constituents
12 are typically nonlinear in the speed [Lozano et al., 1996; Galanis et al., 2005], so the space or
13 time average flux is not generally equal to the flux that would be diagnosed from the averaged
14 current speed. In fact, the average flux will generally depend on higher-order moments of the
15 current speed, such as the standard deviation, skewness, and kurtosis. From both diagnostic and
16 modeling perspectives, there is a need for parameterizations of the probability distribution
17 function (PDF) of the current speed w (called w -PDF here).

18 The w -PDF has been investigated thoroughly in the atmosphere. For example, the w -
19 PDF for the surface winds is well represented by the two-parameter Weibull distribution [e.g.,
20 Monahan, 2006]. However, the w -PDF has not been investigated in the oceans. To fill this gap,
21 we use hourly Acoustic Doppler Current Profiler (ADCP) data (1990-2007) at all the six stations
22 during the Tropical Atmosphere Ocean (TAO) project [McPhaden et al., 1998] in this study to
23 construct the observational w -PDF for various layers. The purpose is to identify which

1 theoretical PDF should be used for the current speed for general and/or special events such as El
2 Nino and La Nina. Special characteristics of the statistical parameters such as mean, standard
3 deviation, skewness, and kurtosis will also be identified. The rest of the paper is organized as
4 follows. Section 2 describes the data. Section 3 presents theoretical background for determining
5 the w -PDF for upper oceans. Section 4 shows the basic characteristics of the four parameters of
6 the Weibull distribution. Section 5 constructs the observational w -PDF from the TAO-ADCP
7 data and discusses the basic features of the four parameters. Section 6 presents the conclusions.

8 **2. Data**

9 The upper layer ocean current dataset consists of hourly ADCP moorings from the TAO
10 project at the six stations (147° E, 156° E, 165° E, 170° W, 140° W, 110° W) along the equator with
11 the vertical resolution of 5 m. Temporal data coverage varies from station to station. 1993-2004
12 with interruptions during 1997-1998 and 2001-2003 on 147° E, 1990-1995 on 156° E, 1990-2007
13 with interruption during 1993-1994 on 165° E, 1999-2006 with interruption 1992-1993 on
14 170° W, 1995-2007 on 140° W, and 1995-2007 with interruption in 2004 on 110° W. The hourly
15 horizontal velocity data (u , v) can be downloaded from the website:
16 <http://www.pmel.noaa.gov/tao/>. The current speed (w) is calculated from (u , v).

17 **3. Theoretical Background**

18 Let (x, y) be the horizontal coordinates and z be the vertical coordinate. The
19 corresponding horizontal velocity components are represented by (\tilde{u}, \tilde{v}) . Large-scale horizontal
20 momentum equation is written by

$$21 \quad \frac{\partial \tilde{u}}{\partial t} - f(\tilde{v} - v_g) = \frac{1}{\rho} \frac{\partial X}{\partial z}, \quad (1)$$

$$22 \quad \frac{\partial \tilde{v}}{\partial t} + f(\tilde{u} - u_g) = \frac{1}{\rho} \frac{\partial Y}{\partial z}, \quad (2)$$

1 where (X, Y) are the horizontal stresses; p is the pressure; ρ is the density; f is the Coriolis
 2 parameter; and (u_g, v_g) are geostrophic velocity components defined by

$$3 \quad u_g = -\frac{1}{f\rho} \frac{\partial p}{\partial y}, \quad v_g = \frac{1}{f\rho} \frac{\partial p}{\partial x}. \quad (3)$$

4 Integrating (1) and (2) from the ocean surface ($z = 0$) to a constant scale depth (h) of surface
 5 mixed layer leads to

$$6 \quad \frac{\partial U}{\partial t} - fV_E = \frac{1}{\rho} (X_0 - X_{-h}), \quad (4)$$

$$7 \quad \frac{\partial V}{\partial t} + fU_E = \frac{1}{\rho} (Y_0 - Y_{-h}), \quad (5)$$

8
 9 where

$$10 \quad (U, V) = \int_{-h}^0 (\tilde{u}, \tilde{v}) dz = (hu, hv), \quad (6)$$

$$11 \quad (U_E, V_E) = \int_{-h}^0 (\tilde{u} - u_g, \tilde{v} - v_g) dz, \quad (7)$$

12
 13 with (u, v) the vertical means of (\tilde{u}, \tilde{v}) , $(X_0, Y_0) = (\tau_x, \tau_y)$ the surface wind stress components;
 14 and (X_{-h}, Y_{-h}) the stress components at $z = -h$, which is calculated by

$$15 \quad \frac{X_{-h}}{\rho} \approx -\frac{K}{h} u, \quad \frac{Y_{-h}}{\rho} \approx -\frac{K}{h} v. \quad (8)$$

16 Here, we assume that the horizontal velocity is much weaker below the mixed layer than in the
 17 mixed layer. K is the eddy viscosity. Substitution of (6)-(8) into (4) and (5) gives

$$18 \quad \frac{\partial u}{\partial t} = \frac{1}{h} \Lambda_u - \frac{K}{h^2} u, \quad (9)$$

$$19 \quad \frac{\partial v}{\partial t} = \frac{1}{h} \Lambda_v - \frac{K}{h^2} v, \quad (10)$$

20 where

$$\Lambda_u \equiv fV_E + \frac{\tau_x}{\rho}, \quad \Lambda_v \equiv -fU_E + \frac{\tau_y}{\rho} \quad (11)$$

represent the residual between the Ekman transport and surface wind stress. With absence of horizontal pressure gradient, e.g., $u_g = v_g = 0$, Equations (9) and (10) reduce to the commonly used wind-forced slab model [e.g., Pollard and Millard, 1970],

$$\frac{\partial u}{\partial t} = fv + \frac{\tau_x}{\rho h} - \frac{K}{h^2} u$$

$$\frac{\partial v}{\partial t} = -fu + \frac{\tau_y}{\rho h} - \frac{K}{h^2}v.$$

For the sake of convenience, we assume that the residual between the Ekman transport (U_E , V_E) and surface wind stress does not depend on the horizontal current vector (u , v). Away from the equator, this approximation is similar to a small Rossby number approximation [Gill, 1982]. If the forcing (Λ_u , Λ_v) is fluctuating around some mean value,

$$\Lambda_u(t) = \langle \Lambda_u \rangle + \dot{W}_1(t) h \Sigma, \quad \Lambda_v(t) = \langle \Lambda_v \rangle + \dot{W}_2(t) h \Sigma, \quad (12)$$

12 where the angle brackets represent ensemble mean and the fluctuations are taken to be isotropic
 13 and white in time:

$$\left\langle \dot{W}_i(t_1) \dot{W}_j(t_2) \right\rangle = \delta_{ij} \delta(t_1 - t_2), \quad (13)$$

with a strength that is represented by Σ . Note that the Ekman transport is determined by the surface wind stress for time-independent case, and therefore the ensemble mean values of (Λ_u, Λ_v) are zero,

$$\langle \Lambda_u \rangle = 0, \quad \langle \Lambda_v \rangle = 0. \quad (14)$$

19 Substitution of (12)-(14) into (9) and (10) gives

$$\frac{\partial u}{\partial t} = -\frac{K}{h^2} u + \dot{W}_1(t) \Sigma, \quad (15)$$

$$\frac{\partial v}{\partial t} = -\frac{K}{h^2} v + \dot{W}_2(t) \Sigma, \quad (16)$$

3 which is a set of stochastic differential equations for the surface current vector. The joint PDF of
 4 (u, v) satisfies the Fokker-Planck equation,

$$\frac{\partial p}{\partial t} = \left(\frac{\Sigma^2}{2} \right) \left(\frac{\partial^2 p}{\partial u^2} + \frac{\partial^2 p}{\partial v^2} \right) + \frac{\partial}{\partial u} \left[\left(\frac{K}{h^2} u \right) p \right] + \frac{\partial}{\partial v} \left[\left(\frac{K}{h^2} v \right) p \right], \quad (17)$$

6 which is a linear second-order partial differential equation with the depth scale (h) taken as a
 7 constant. Transforming from the orthogonal coordinates (u, v) to the polar coordinates (w, φ)
 8 respectively the current speed and direction,

$$u = w \cos \varphi, \quad v = w \sin \varphi. \quad (18)$$

10 The joint PDF of (u, v) is transformed into the joint PDF of (w, φ) ,

$$p(u,v)dudv = p(u,v)wdwd\varphi = \tilde{p}(w,\varphi)dwd\varphi. \quad (19)$$

12 Integration of (19) over the angle φ from 0 to 2π yields the marginal PDF for the current speed
 13 alone,

$$p(w) = \int_0^{2\pi} \tilde{p}(w, \varphi) d\varphi . \quad (20)$$

15 For a constant eddy viscosity (K) at $z = -h$, the steady state solution of equation (17) is given by

$$p(u, v) = A \exp\left[-\frac{K}{\Sigma^2 h^2}(u^2 + v^2)\right], \quad (21)$$

where A is a normalization constant. Substitution of (21) into (19) and use of (20) yield

$$p(w) = 2\pi A w \exp\left(-\frac{Kw^2}{\Sigma^2 h^2}\right), \quad (22)$$

19 with

$$\int_0^\infty p(w)dw = 1. \quad (23)$$

1 Substitution of (22) into (23) leads to the Rayleigh distribution

2

$$p(w) = \frac{2w}{a^2} \exp\left[-\left(\frac{w}{a}\right)^2\right], \quad a \equiv \frac{\Sigma h}{\sqrt{K}}, \quad (24)$$

3 with the scale parameter a . The basic postulation of constant K may not be met always at the
 4 upper ocean. Hence we require a model that can meet the twin objectives of (a) accommodating
 5 Rayleigh distribution whenever the basic hypothesis (constant K) that justifies it is satisfied and
 6 (b) fitting data under more general conditions. This requirement is supposed to be satisfied by the
 7 Weibull probability density function,

8

$$p(w) = \frac{b}{a} \left(\frac{w}{a}\right)^{b-1} \exp\left[-\left(\frac{w}{a}\right)^2\right], \quad (25)$$

9 where the parameters a and b denote the scale and shape of the distribution. This distribution has
 10 been recently used in investigating the ocean model predictability by Ivanov and Chu [2007 a,
 11 b].

12 4. Parameters of Weibull Distribution

13 The four parameters (mean, standard deviation, skewness, and kurtosis) of the Weibull
 14 distribution are calculated by [Johnson et al., 1994]

15

$$\text{mean}(w) = a \Gamma\left(1 + \frac{1}{b}\right), \quad (26)$$

16

$$\text{std}(w) = a \left[\Gamma\left(1 + \frac{2}{b}\right) - \Gamma^2\left(1 + \frac{1}{b}\right) \right]^{1/2}, \quad (27)$$

17

$$\text{skew}(w) = \frac{\Gamma\left(1 + \frac{3}{b}\right) - 3\Gamma\left(1 + \frac{1}{b}\right)\Gamma\left(1 + \frac{2}{b}\right) + 2\Gamma^3\left(1 + \frac{1}{b}\right)}{\left[\Gamma\left(1 + \frac{2}{b}\right) - \Gamma^2\left(1 + \frac{1}{b}\right) \right]^{3/2}}, \quad (28)$$

1 $\text{kurt}(w) = \frac{\Gamma\left(1+\frac{4}{b}\right) - 4\Gamma\left(1+\frac{1}{b}\right)\Gamma\left(1+\frac{3}{b}\right) + 6\Gamma^2\left(1+\frac{1}{b}\right)\Gamma\left(1+\frac{2}{b}\right) - 3\Gamma^4\left(1+\frac{1}{b}\right)}{\left[\Gamma\left(1+\frac{2}{b}\right) - \Gamma^2\left(1+\frac{1}{b}\right)\right]^2} - 3, \quad (29)$

2 where Γ is the gamma function. The parameters a and b can be inverted [Monahan, 2006] from
 3 (26) and (27),

4 $b \approx \left[\frac{\text{mean}(w)}{\text{std}(w)} \right]^{1.086}, \quad a = \frac{\text{mean}(w)}{\Gamma(1+1/b)}. \quad (30)$

5 The skewness and kurtosis depend on the parameter b only [see (26) and (27)] for the Weibull
 6 distribution. The relationship between the kurtosis and skewness can be determined from (28)
 7 and (29).

8 **5. Observational w -PDFs**

9 The data depicted in Section 2 are used to construct observational w -PDF (i.e.,
 10 histograms) for the two stations (165°E , 110°W) along the equator in upper oceans (0 - 50 m) for
 11 the whole period (1990-2007), major El Nino events (May 91-Jul 92, Dec 92-Jun 93, Jul 94-Mar
 12 95, May 97-Apr 98, May 02-Mar 03, Jul 04-Feb 05, Sep 06-Jan 07), and major La Nina events
 13 (Sep 95-Mar 96, Jul 98-Jun 00, Oct 00-Feb 01, Aug-Dec 07). It is found that the observational
 14 w -PDF fit the two-parameter Weibull distribution reasonably well in all occasions (Fig. 1). At
 15 165°E (western Pacific) the w -PDF has a largest peakedness with a lower mode (0.25 m s^{-1})
 16 during the La Nina events, a medium peakedness for the whole period, and smallest peakedness
 17 with a higher mode (0.4 m s^{-1}) during the El Nino events; and vice versa at 110°W (eastern
 18 Pacific), the w -PDF has a largest peakedness with a lower mode (0.4 m s^{-1}) during the El Nino
 19 events, a medium peakedness for the whole period, and smallest peakedness with a higher mode
 20 (0.65 m s^{-1}) during the La Nina events. From the western to eastern Pacific, the mode is

1 comparable (0.4 m s^{-1}) during the El Nino events, and increases from 0.25 m s^{-1} to 0.65 m s^{-1}
 2 during the La Nina event. Such flip pattern of w -PDF between the eastern and western Pacific
 3 during El Nino/La Nina events may imply the importance of equatorial current systems in the El
 4 Nino-Southern Oscillation phenomenon.

5 The four parameters (mean, standard deviation, skewness, and kurtosis) can also be
 6 calculated from the observational data (w),

$$7 \quad \text{mean}(w) = \frac{1}{N} \sum_{i=1}^N w_i, \quad \text{std}(w) = \sqrt{\text{mean}[(w - \text{mean}(w))^2]},$$

$$8 \quad \text{skew}(w) = \frac{\text{mean}\{[(w - \text{mean}(w))^3]\}}{\text{std}^3(w)}, \quad \text{kurt}(w) = \frac{\text{mean}\{[(w - \text{mean}(w))^4]\}}{\text{std}^4(w)} - 3, \quad (31)$$

9 for any location (station, depth) where the ADCP measurements were taken. Thus, a four-
 10 parameter dataset has been established each location. The scatter diagrams are drawn for all six
 11 stations (147°E , 156°E , 165°E , 170°W , 140°W , and 110°W) along the equator in upper oceans (0
 12 - 50 m) and sub-layer (100 - 200 m) for the whole period (1990-2007), and El Nino/La Nina
 13 events. We may use the relationships between the skewness and the mean/std ratio (representing
 14 the parameter b , Fig. 2) and between the kurtosis and the skewness (Fig. 3) to identify the fitness
 15 of the Weibull distribution for observational w -PDFs for the whole period and the El Nino/La
 16 Nina events. The solid curve on these figures shows the relationship for a Weibull variable.

17 For the observational w -PDF in the upper layer (0 - 50 m), the $\text{skew}(w)$ is evidently a
 18 concave function of the ratio $\text{mean}(w)/\text{std}(w)$ (the same as the Weibull distribution), such that the
 19 theoretical function is positive for small values of this ratio and negative for large values.
 20 However, the ratio $\text{mean}(w)/\text{std}(w)$ is always less than 2 for the whole period and El Nino
 21 events, and less than 2.5 for the La Nina events. The skewness is generally positive in the upper
 22 tropical Pacific for all occasions (Fig. 2, upper panel). Similarly, the relationship between

1 skew(w) and kurt(w) in the observations is also similar to that for a Weibull variable (Fig. 3).
2 The agreement between the moment relationships in the upper layer (0-50 m) TAO-ADCP data
3 and those for a Weibull variable reinforces the conclusion that these data are Weibull to a good
4 approximation, which is not affected by the large-scale processes such as El Nino and La Nina
5 events.

6 The scatter diagrams of skew(w) versus ratio mean(w)/std(w) and kurt(w) versus skew(w)
7 for the sub-layer (100 - 200 m) (lower panels of Figs. 2 and 3) show that the w -PDF for the lower
8 layer (100-200 m) does not fit the Weibull distribution so well as the upper layer. Evident
9 difference is found between the observational w -PDF and the Weibull distribution. Such
10 difference can be explained as follows. For the upper layer, the horizontal velocity satisfies (9)
11 and (10). This leads to the current speed (w) satisfies the Rayleigh distribution for the constant
12 eddy viscosity K and may extend to more general Weibull distribution for non-constant K . For
13 the lower layer, the horizontal velocity does not satisfy (9) and (10). This may cause the
14 deviation of w -PDF from the Weibull distribution.

15 **6. Conclusions**

16
17 This study has investigated the probability distribution function of the current speeds (w)
18 in upper tropical Pacific observationally, using long-term (1990-2007) hourly Acoustic Doppler
19 Current Profiler (ADCP) data at six stations during the Tropical Atmosphere Ocean (TAO)
20 project; and theoretically, using a stochastic model derived using boundary layer physics. The
21 following results were obtained.

22 (1) Probability distribution function of the current speeds (w) satisfies the two-parameter
23 Weibull distribution in the upper tropical Pacific Ocean (0 - 50 m) and does not satisfy the two-
24 parameter Weibull distribution in lower tropical Pacific (100-200 m). In the upper tropical

1 Pacific with a constant eddy viscosity K , the probability distribution function satisfies a linear
2 second-order partial differential equation (i.e., the Fokker-Planck equation) with an analytical
3 solution – the Rayleigh distribution (special case of the 2 parameter Weibull distribution). The
4 stochastic differential equations are different between upper and lower layers in tropical Pacific
5 (i.e., making the corresponding Fokker-Planck equation different), which causes the probability
6 distribution function different.

7 (2) The w -PDF in the upper ocean (0 - 50 m) satisfies the two-parameter Weibull
8 distribution reasonably well all the time with different characteristics between El Nino and La
9 Nina events. In the western Pacific, the w -PDF has a larger peakedness during the La Nina
10 events than during the La Nino events; and vice versa in the eastern Pacific. From the western to
11 eastern Pacific, the mode is comparable (0.4 m s^{-1}) during the El Nino events, and increases from
12 0.25 m s^{-1} to 0.65 m s^{-1} during the La Nino event. Such flip pattern of w -PDF between the
13 eastern and western Pacific during El Nino/La Nina events may imply the importance of
14 equatorial current systems in the El Nino-Southern Oscillation phenomenon.

15 (3) Four moments of w (mean, standard deviation, skewness, kurtosis) have been
16 characterized. It was found that the relationships between $\text{mean}(w)/\text{std}(w)$ and $\text{skew}(w)$ and
17 between $\text{skew}(w)$ and $\text{kurt}(w)$ from the data are in fairly well agreement with the theoretical
18 Weibull distribution for the upper (0 - 50 m) tropical Pacific for the whole period as well as El
19 Nino/La Nina events, but are not in well agreement with the theoretical Weibull distribution for
20 the lower (below 100 m depth) tropical Pacific. The ADCP data also show that the ratio
21 $\text{mean}(w)/\text{std}(w)$ is generally less than 2 for the whole period and El Nino events, and less than
22 2.5 for the La Nino events. The skewness is generally positive in the upper (0 - 50 m) tropical
23 Pacific.

1 (4) A primary motivation for the study of the probability distribution of upper layer ocean
2 current speeds is the role these distributions play in the computation of spatially and/or
3 temporally averaged horizontal fluxes of momentum, heat, water mass and chemical
4 constituents. The Weibull distribution provides a good empirical approximation to the PDF of w ,
5 which is not affected by the large-scale processes such as El Nino and La Nina events. This
6 presents the possibility of improving the representation of the horizontal fluxes that are at the
7 heart of the coupled physical–biogeochemical dynamics of the marine system.

8 **Acknowledgments**

9 The author would like to thank Mr. Chenwu Fan for invaluable comments and
10 computational assistance, and the TAO Project Office of NOAA/PMEL for providing the ADCP
11 data in tropical Pacific along the equator. The Office of Naval Research, Naval Oceanographic
12 Office, and Naval Postgraduate School sponsored this research.

13 **References**

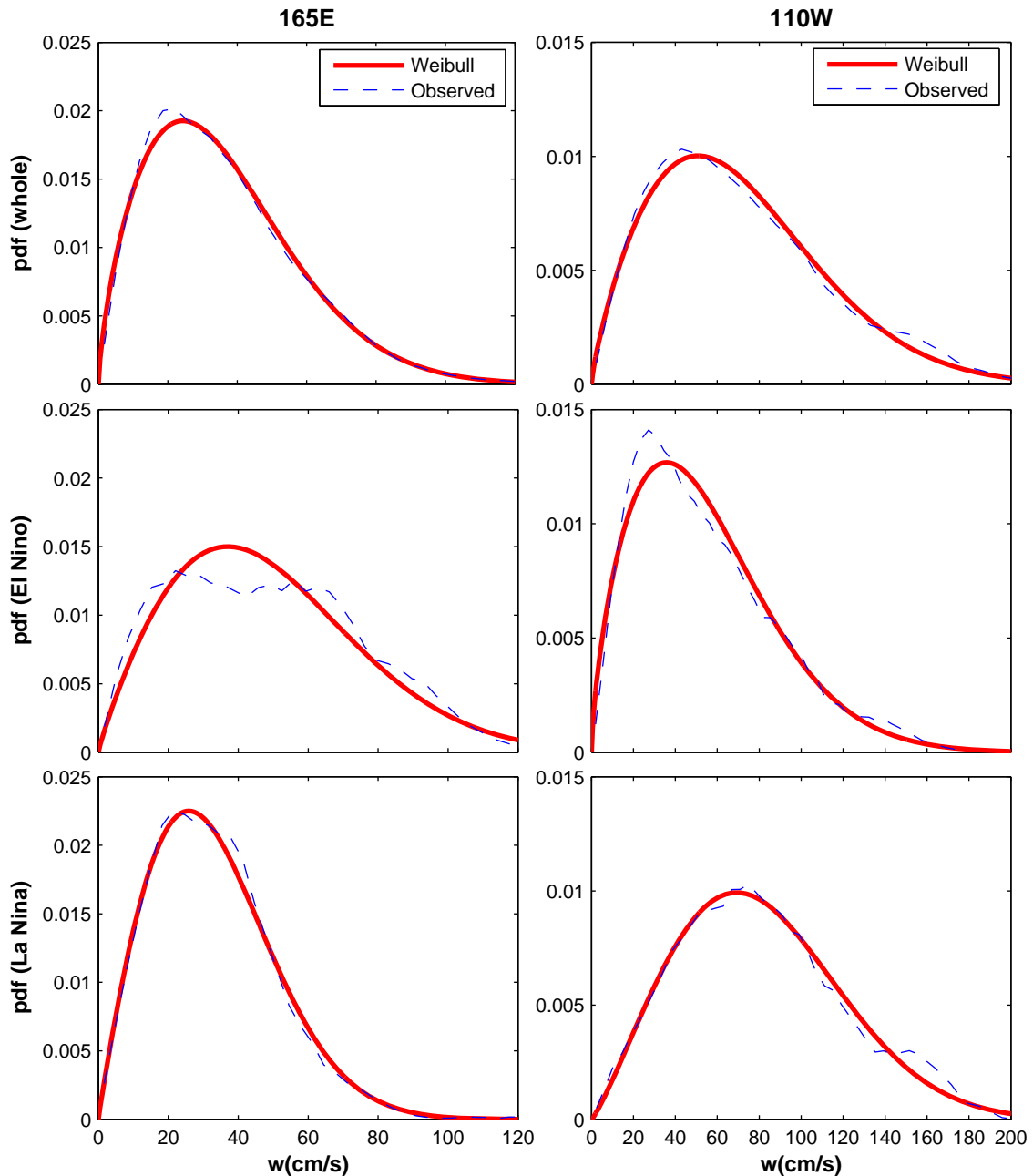
- 14 Galanis, G., P. Louka, P. Katsafados, G. Kallos I. Pytharoulis, Applications of Kalman filters
15 based on non-linear functions to numerical weather predictions. *Ann. Geophys.*, **24**, 2451-2460,
16 2005.
- 17
- 18 Gill, A.E., *Atmosphere-Ocean Dynamics*, Academic Press, San Diego, 662 pp, 1982.
- 19
- 20 Ivanov, L. M., and P.C. Chu, 2007: On stochastic stability of regional ocean models to finite-
21 amplitude perturbations of initial conditions. *Dyn. Atmos. Oceans*, **43**, 199-225,
22 doi:10.1016/j.dynatmoce.2007.03.001, 2007a.
- 23

- 1 Ivanov, L. M., and P.C. Chu, On stochastic stability of regional ocean models with uncertainty in
2 wind forcing. *Nonlinear Proc. Geophys.*, 14, 655-670, 2007b.
- 3
- 4 Johnson, N., S. Kotz, and N. Balakrishnan, *Continuous Univariate Distributions*. Vol. 1. Wiley,
5 756 pp, 1994.
- 6
- 7 Lozano, C. J., A.R. Robinson, H.G. Arrango, A. Gangopadhyay, Q. Sloan, P. J. Haley, L.
8 Anderson, and W. Leslie, An interdisciplinary ocean prediction system: assimilation strategies and
9 structured data models. In: *Modern Approaches to Data Assimilation in Ocean Modeling*, edited
10 by P. Malanotte-Rizzoli, Elsevier, Amsterdam, 1996.
- 11
- 12 Monahan, A. H., The probability distribution of sea surface wind speeds. Part-1: theory and
13 SeaWinds observations. *J. Climate*, **19**, 497-519. 2006.
- 14
- 15 McPhaden, M.J., A.J. Busalacchi, R. Cheney, J.R. Donguy, K.S. Gage, D. Halpern, M. Ji, P.
16 Julian, G. Meyers, G.T. Mitchum, P.P. Niiler, J. Picaut, R.W. Reynolds, N. Smith, and K.
17 Takeuchi, The Tropical Ocean-Global Atmosphere (TOGA) observing system: A decade of
18 progress. *J. Geophys. Res.*, **103**, 14,169–14,240, 1998.
- 19
- 20 Pollard, R. T., and R. C. Millard, Comparison between observed and simulated wind-generated
21 inertial oscillations, *Deep Sea Res.*, **17**, 795-812, 1970.

1

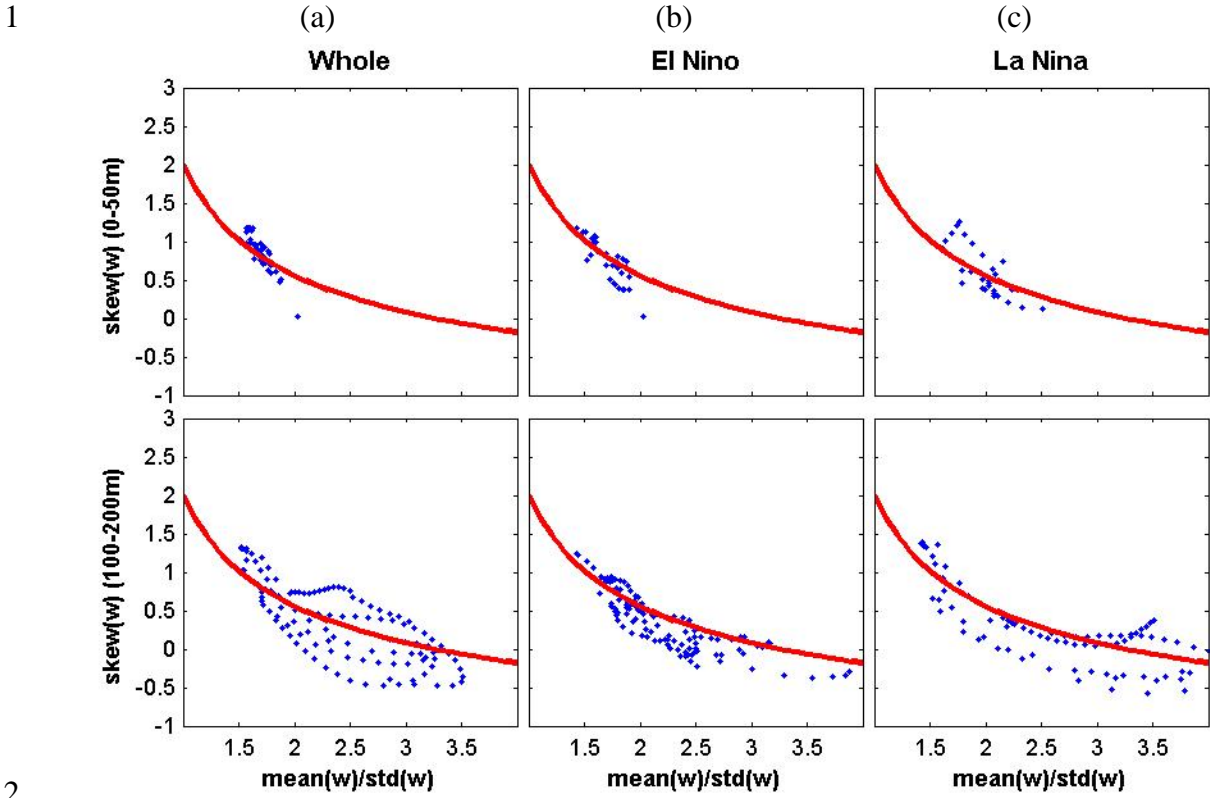
(a)

(b)



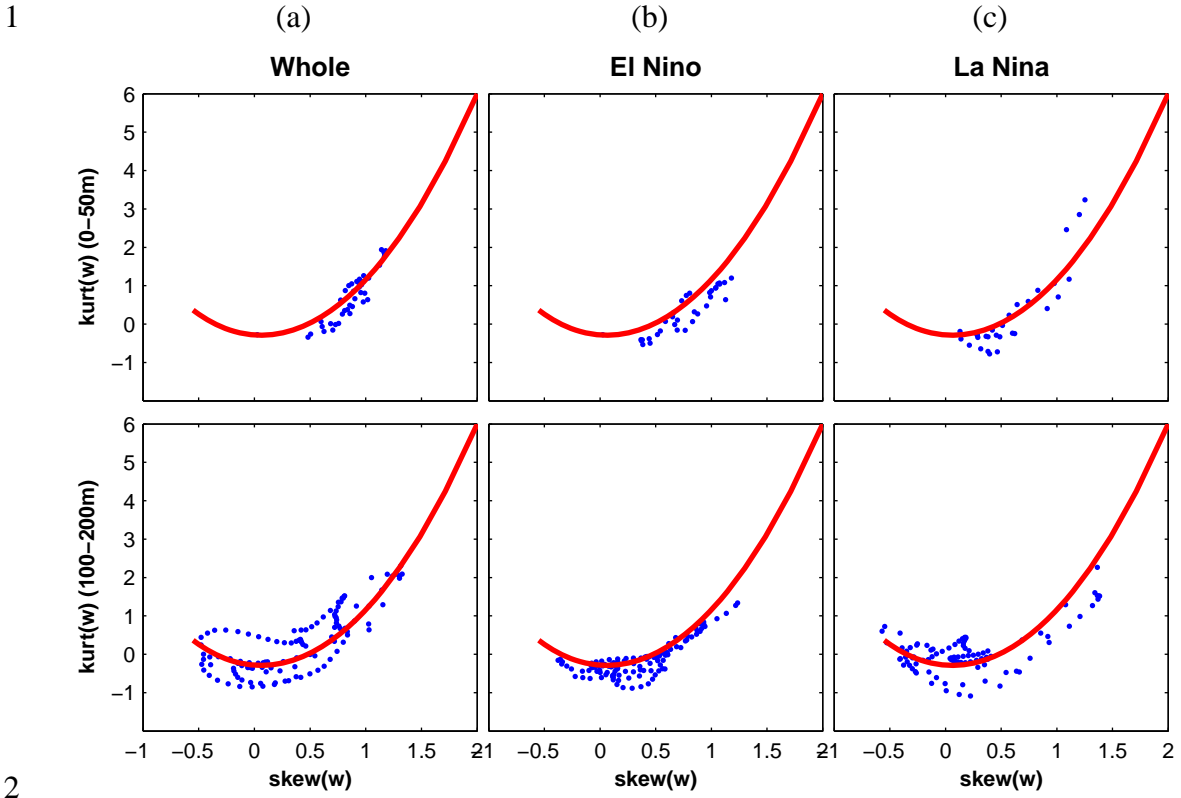
2

3 Fig. 1. Comparison between observational w -PDFs (i.e., histogram, dashed curve) constructed
 4 from the TAO-ADCP data and Weibull distributions (solid curve) for upper layer (0-50 m)
 5 along the equator at: (a) 156°E , and (b) 110°W with the upper panels for the whole period, the
 6 middle panels for the major El Nino events, and the lower panels for the major La Niña events.



2
3
4 Fig. 2. Relationship between the ratio $\text{mean}(w)/\text{std}(w)$ and $\text{skew}(w)$ for the observational w -PDFs
5 (dots) from TAO-ADCP at the six stations and the Weibull distribution (solid curve) during (a)
6 the whole period, (b) major El Nino events, and (c) major La Nina events with the upper panels
7 for the upper layer (0-50 m), and the lower panels for the sub-layer (100-200 m).

8



4 Fig. 3. Relationship between $\text{kurt}(w)$ and $\text{skew}(w)$ for the observational w -PDFs (dots) from
 5 TAO-ADCP at the six stations and the Weibull distribution (solid curve) during (a) the whole
 6 period, (b) major El Nino events, and (c) major La Nina events with the upper panels for the
 7 upper layer (0-50 m), and the lower panels for the sub-layer (100-200 m).

